

Fabricating a Low-Cost Raman Spectrometer to Introduce Students to Spectroscopy Basics and Applied Instrument Design

Neethu Emmanuel, Raji B Nair, Bini Abraham, and Karuvath Yoosaf*

 Cite This: *J. Chem. Educ.* 2021, 98, 2109–2116

 Read Online

ACCESS |

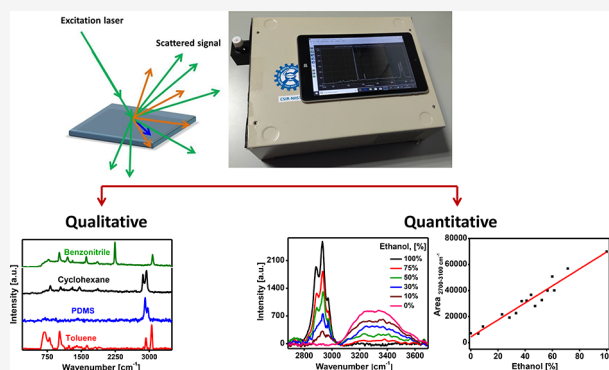
 Metrics & More

 Article Recommendations

 Supporting Information

ABSTRACT: Raman spectroscopy has become a popular analytical tool because of its ability to probe nondestructively and provide fingerprint information about materials. The advancements in the field of Raman spectroscopy and the expanding scope of applications warrant the introduction of the topic in the formal education curriculum. The introduction of Raman spectroscopy analysis in the educational curriculum helps the students learn the spectroscopy basics. Furthermore, component-wise familiarization and fabrication training will help the students to evolve their own methodologies to fabricate and customize the instrument for specific applications. Though many Raman spectrometers are commercially available, the high cost makes it unaffordable for most academic institutions. Herein, we describe an easy and cost-effective method to make a fully integrated portable Raman spectrometer and explain a few simple experiments which can be conducted at the classroom level using the fabricated device.

KEYWORDS: Graduate Education/Research, Analytical Chemistry, Demonstrations, Physical Chemistry, Laboratory Equipment/Apparatus, Qualitative Analysis, Quantitative Analysis, Raman Spectroscopy, Spectroscopy



INTRODUCTION

Raman spectroscopy (RS), based on the concept of inelastic scattering invented by C.V. Raman,¹ provides fingerprint vibrational information and serves as a nondestructive technique for the reliable identification of substances. In contrast with absorption-based IR spectroscopy, RS relies on scattering, offering considerable flexibility to both instrumental designs and sample handling. With the advent of new generation lasers and optical components, Raman spectra can currently be acquired even with handheld and battery-operable systems, which have elevated their potential for onsite and point of care applications. Due to minimal interference from water, RS is suitable for studying biological samples even in their native state. RS has evolved as a preferable analytical tool in numerous areas like medical diagnosis,^{2,3} pharmaceutical and food industries,^{4,5} environmental quality testing,⁶ forensics,⁷ homeland security,⁸ anticounterfeiting,⁹ archeology,¹⁰ geology,¹¹ gemstone purity checking,^{12,13} etc., surpassing the limitations of other spectroscopic techniques. This has necessitated introducing RS as an important spectroscopic technique in the formal education curriculum. RS could be introduced to undergraduate students for enhancing their fundamental understanding of spectroscopic techniques through representative examples with various objectives. For example, combining computational chemistry with vibrational spectroscopy experiments is useful for imparting the concepts

of symmetry, polarizability, and selection rules.^{14,15} In the field of practical analytical chemistry, Raman spectrometers are introduced for material identification, mixture analysis,¹⁶ and quantification.¹⁷ In biochemistry, RS helps to characterize cell membranes¹⁸ and demonstrate the potential of multivariate tools for estimating the biomolecular concentrations from complex mixtures.¹⁹ In the emerging fields of nanoscience and nanotechnology,^{20,21} students can characterize and estimate purity and the number of layers of laboratory prepared 2D nanomaterials like graphenes.²² Laboratory experiments can be conducted to teach the concept of surface enhanced Raman spectroscopy (SERS), calculate the enhancement factors, study influences of nanomaterial size and shape,^{20,23} and demonstrate the practical utility of SERS to trace level analyte detection,²⁴ colorants in precious artworks,²⁵ etc. These teaching experiments are augmented by the availability of cost-effective Raman spectrometers at educational institutions easily accessible to students. In addition, knowing the working principles of the instrument and functionalities of each of the

Received: August 5, 2020

Revised: April 11, 2021

Published: May 3, 2021



Table 1. Synopsis of Significant Contributions in the Literature for Cost-Effective Solutions for Raman Spectrometers

literature source	laser used	probe optics used	detector used	approximate cost, \$U.S.
Gallow et al. ^a	nitrogen laser: 337.2 nm	90°	PMT-based monochromator	not available
Sutherland et al. ^b	He–Ne laser: 9 mW	direct mode	APD-based monochromator	not available
Fitzwater et al. ^c	He–Ne laser: 632.8 nm, 10 mW	90°	PMT-based monochromator	20,000
Bandyopadhyay et al. ^d	argon laser: 514.5 nm, 4 W	backscattering configuration with small-sized mirror as the beam splitter and notch filter	PMT-based monochromator	not available
DeGraff et al. ^e	532 nm, 10 mW	90° probe with notch filter	Ocean Optics S2000	5000
Young et al. ^f	green laser pointer: 532 nm, ~20 mW	backscattering 200 μm core reflection fiber-optic probe and notch filter	Ocean Optics SD2000	3700
Johnson et al. ^g	532 nm, 20 mW	~45° probe optics, notch filter	Ocean Optics HR2000	6500
Mohr et al. ^h	laser pointer: 532 nm, 4 mW	backscattering with a small mirror beam splitter, notch filter	CCD array detector	5000
Somerville et al. ⁱ	laser pointer: 532 nm, 5 mW; He–Ne laser: 633 nm, 30 mW	90° and backscattering, edge filter	Ocean Optics HR4000	3000
Rossi et al. ^j	laser pointer: 532 nm, < 100 mW	transmission mode with Raman edge filter	digital camera 3D printed case	3000
present work	laser pointer: 532 nm	backscattering probe, colored glass long-pass filter	Science Surplus	700 ^k
present work	Thorlabs DJ532–40: 532 nm, ~40 mW	backscattering probe, colored glass long-pass filter	Science-Surplus	970 ^k
present work	laser pointer: 532 nm	backscattering probe, colored glass long-pass filter	home-built spectrometer	940 ^k
present work	laser pointer: 532 nm	backscattering probe, colored glass long pass filter	Ocean Optics USB4000	4000 ^k
present work	laser pointer: 532 nm	backscattering probe, colored glass long-pass filter	Thunder Optics	700 ^k
present work	laser pointer: 532 nm	backscattering probe, colored glass long-pass filter	Thorlabs CCS100	2700 ^k

^aSee ref 26. ^bSee ref 27. ^cSee ref 28. ^dSee ref 29. ^eSee ref 30. ^fSee ref 31. ^gSee ref 32. ^hSee ref 33. ⁱSee ref 34. ^jSee ref 35. ^kSee the Supporting Information for more detail on costs.

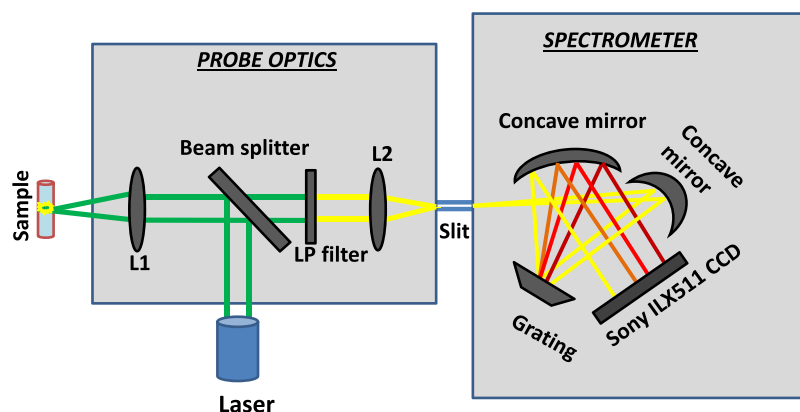


Figure 1. Schematic layout of the portable Raman spectrometer.

components will help the students evolve their own methodologies to fabricate and customize for specific applications.

Commercially available Raman spectrometers cost a minimum of \$12,000 U.S. and are thus unaffordable by most schools and colleges. There have been several efforts to provide cost-effective solutions for RS, and significant contributions are listed in Table 1. Most of these demonstrated configurations provide flexibility in connecting collection optics via optical fiber with any commercial detectors available in the educational institutes. On the other hand, the free-space coupling of the output of the collection optics to the detector may avoid fiber coupling and transmission losses, allowing the detection of less intense signals yielding improved sensitivity. A fully integrated and battery-operable system will also be handier and easy to carry to the point of requirement. Primarily, the availability of such systems will help teaching theory along with

the parallel demonstration of analytical concepts. Herein, we outline a detailed method of constructing a fully integrated and cost-effective portable Raman spectrometer. Furthermore, we describe the functions of different components and how their technical specification can influence the acquired data.

EXPERIMENTAL SECTION

Optical Configuration

Figure 1 displays the adopted optical layout of the device. Herein, we used a JD-851 green laser pointer as the excitation source, probe optics with backscattering configuration, and a Science-Surplus spectrometer as the detector. A power bank (portable mobile charger) is used to supply power for both the laser diode and the spectrograph. The spectral acquisition and display are made on an 8-in. tablet with Windows OS. A

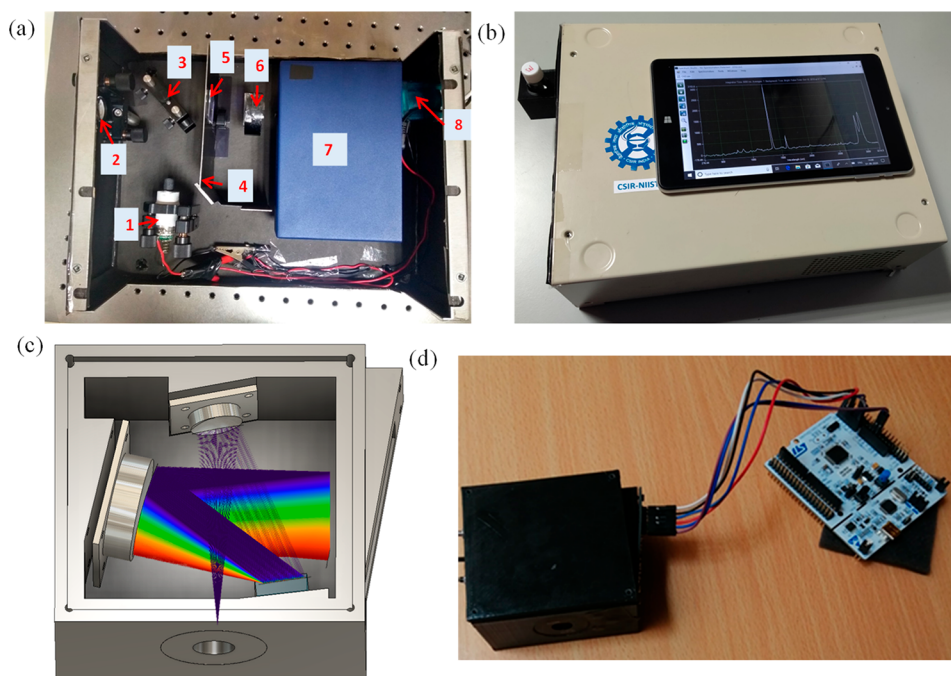


Figure 2. Photographs showing (a) internal components: (1) laser diode, (2) focusing lens, (3) beam splitter, (4) plate to block ambient light and reflected laser entering detector unit, (5) long-pass filter, (6) focusing lens, (7) spectrometer, and (8) RS232 to USB converter to communicate with a Windows tablet. (b) External view of the device showing the 3D printed sample holder and the Windows tablet for spectral acquisition and display, (c) 3D design of the spectrometer, and (d) in-house fabricated spectrometer along with STM32 Nucleo board.

detailed component-wise description and fabrication procedure are explained in the following sections.

Excitation Source

The excitation source's technical specifications, such as wavelength, line width (monochromaticity), optical power, etc., are crucial for obtaining good quality Raman spectra. Typically, the Raman spectrum appears ~ 10 – 200 nm above (Stokes) and below (anti-Stokes) the excitation wavelength. The Raman scattering efficiency varies inversely to the fourth power of the excitation wavelength.³⁶ Thus, lasers with lower excitation wavelength (UV and visible) produce a better Raman signal than the IR light sources. We have used a low-cost and readily available green (~ 532 nm) laser pointer JD-851, a diode pumped solid state laser (DPSS), as the excitation source. The inbuilt Nd:YAG and KTP crystals convert the laser diode's primary emission wavelength, 808 nm, first to 1064 nm and then to 532 nm. Favorably, the laser pointers come with the necessary electronic driver circuit, passive heat dissipater, and collimator lens assembly (see [Supporting Information](#)), eliminating the need for additional components. The laser beam diameter is ~ 2.5 mm, and optical output power is ~ 70 mW, which is sufficient to produce an easily detectable amount of Raman scattered photons. The measured spectral profile indicated that the central wavelength and FWHM are 531.8 nm and ~ 0.78 nm, respectively (see [Supporting Information](#)). From this, the minimum achievable Raman spectral resolution is estimated to be in the range of 20 – 28 cm^{-1} . Corresponding to a 300 – 3000 cm^{-1} Raman shift, the Stokes lines will fall in the range of 540 – 630 nm, and typical silicon detectors exhibit the highest efficiency in this range.³⁷ All these factors contribute to the easy detection of Raman scattered photons with a low-cost CCD detector. Alternatively, one can use commercially available laser diodes like Thorlabs DJS32-40, which also works based on the same principle.

The presence of additional diminished intensity 808 nm lines in the emission profile, generated from the diode within the laser, does not influence the measurement due to the following reasons:

- (i) Its intensity is almost 25 times weaker than the 532 nm.
- (ii) Compared to 532 nm, the 808 nm emission is red-shifted by 276 nm and thus 100 times weaker scattering cross-section.
- (iii) Its Stokes lines appear beyond the sensitive region of the spectrometer.
- (iv) Its anti-Stokes lines appear in the wavelength range 650 – 795 nm, beyond the region of interest.

Probe Optics

The major preferred configurations for probe optics are transmission, 90° , backscattered, and spatially offset. The third is the simplest as it is easy to set up with minimum components and alignment. The primary considerations are to (i) maximize the collection efficiency of the weak Raman radiation and (ii) block the intense Rayleigh radiation from entering into the detection unit. These goals are achieved through focusing lenses, a beam splitter, and a long-pass filter. The collimated light from the laser diode is directed to the sample through a beam splitter and a focusing lens (L1). The purpose of the beam splitter is to separate the excitation light path from the collection path. Instead of specifically designed beam splitters, we used a square cut piece of a microscopic slide (25 mm \times 25 mm \times 1 mm), which, when kept at 45° to the excitation light path, yielded a reflection/transmission ratio of 30:70 (see [Supporting Information](#)). The backscattered radiation is collected by the same lens (L1), and a portion of this beam directly passes through the beam splitter and is focused on the entrance slit of the spectrophotometer by the second focusing lens (L2). Rayleigh scattered light was blocked

using a long-pass filter with a cutoff wavelength at 550 nm kept in between the beam splitter and L2 lens (see [Supporting Information](#))

Detector

The detector used is a Science-Surplus make having a spectral range of $\sim 450\text{--}700\text{ nm}$. However, the present design does not restrict readers from using any other commercially available (e.g., Ocean Optics, Research India, Thunder Optics, etc.) or in-house fabricated spectrometers. The Science-Surplus spectrometer essentially consists of a $50\ \mu\text{m}$ entrance slit, concave mirrors as focusing elements, an 1800 lines/mm diffraction grating, and a Sony ILX511 linear silicon CCD detector. The spectrometer has a resolution of $\sim 1\text{ nm}$, restricting the maximum achievable Raman spectral resolution to $\sim 35\text{ cm}^{-1}$ at 100 cm^{-1} and $\sim 25\text{ cm}^{-1}$ at 3000 cm^{-1} for a 532 nm excitation. The spectrometer was precalibrated in the factory, and the software module has an inbuilt function for recording the spectra in Raman shift mode. Alternatively, the spectrometer can be calibrated individually, and the detailed procedure is provided in the [Supporting Information](#); however, there was hardly any difference.

As an alternative to the commercial spectrometer, we also attempted the feasibility of building a home-built spectrometer for detecting the Raman signal. Kovarik et al. provides a detailed review of different student-built spectrophotometers.³⁸ Herein, we designed and implemented a dispersive spectrometer in Czerny-Turner configuration using the following components:

- (i) $50\ \mu\text{m}$ entrance slit
- (ii) 1200 lines/mm plane-ruled diffraction grating
- (iii) Two concave mirrors, each with 50 mm focal length
- (iv) Toshiba TCD1304 linear CCD
- (v) home-built CCD driver
- (vi) ST Microelectronics Nucleo-F401RE microcontroller

Firmware and the GUI for data acquisition were adopted from Esben Rossel's work.³⁹ The optical configuration was first optimized on an optical breadboard and then translated into a 3D printed enclosure ([Figure 2C](#) and [D](#); see [Supporting Information](#) for more details).

Elimination of Noises

The prominent noises that interfere with the Raman spectrum are (i) high-frequency noises contributed by electronic circuitry and dark current from the detector and (ii) low-frequency noises from fluorescence and stray light. The effect of the former is minimizable by subtracting a blank spectrum (taken with laser off) from the sample spectrum and of the latter through baseline correction using the moving point average algorithm proposed by Krishna et al.⁴⁰

HAZARDS

The laser is a potential hazard if not properly handled; especially, the 70 mW laser is deeply in the class 3B category. It can cause immediate and irreversible eye damage and skin burning due to the localized heat produced.^{41,42} Directly looking into the laser or from reflected surfaces is to be avoided. It is advisable to remove ornaments such as rings, bangles, watches, etc., which may cause unexpected light reflections. Proper safety procedures such as wearing laser goggles (example LOTG-DYE2/CM Newport, OD ~ 4 at 450–585 nm) need to be followed while operating the device. For the alignment, one of the following strategies are

recommended: (i) place a neutral density filter (optical density 2) in front of the laser source, (ii) wear safety goggles having an optical density of 2–3 at 532 nm (e.g., Thorlabs LG14), or (iii) use safety goggles having an optical density of 4 (e.g., LOTG-DYE2/CM, Newport) and follow the beam path using a paper coated with fluorescent material such as rhodamine. Do not allow other personnel to enter the room during the rough stages of alignment. Keep proper beam blocks in place around the instrument, which would protect persons from stray reflections. Gloves and splash goggles should be worn while working with chemicals. Volatile chemicals should be analyzed in capped glass containers. When demonstrating in classrooms, specifically designed sample holders (preferably black colored) should always be used, which confines radiation inside and minimizes reflections. While connecting the electrical cables, always wear gloves. Care must be taken to avoid short-circuiting, overheating, etc.

RESULTS AND DISCUSSION

[Figure 2](#) represents the photographs of the fabricated Raman spectrometer and the home-built detector. The designed mechanical layout, procedures for component integration, and optimization of alignment are detailed in the [Supporting Information](#).

Sample Analysis

Validation of the fabricated device was carried out by analyzing various standard samples and comparing the data with those recorded using a commercial confocal Raman microscope (Model: WITec Alpha300R, M/s WITec Inc. Germany, see [Supporting Information](#) for detailed specifications). As an example, [Figure 3](#) represents the Raman spectrum of various chemicals such as benzonitrile, cyclohexane, polydimethylsiloxane (PDMS), and toluene taken using the fabricated system (see [Supporting Information](#) for data taken using the commercial system). The observed peak positions are

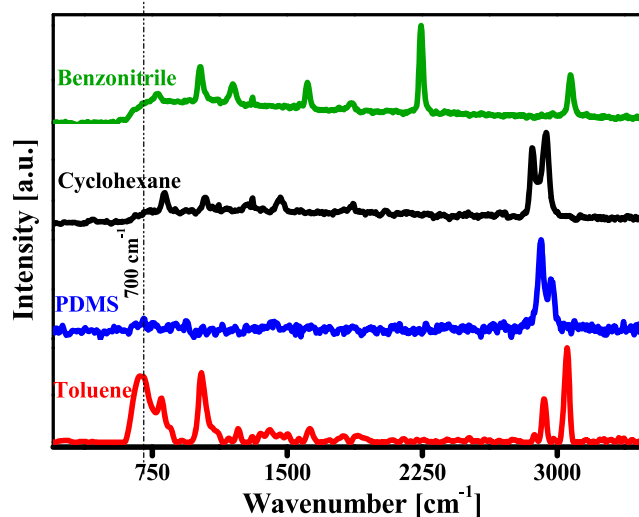


Figure 3. Raman spectra of benzonitrile, cyclohexane, PDMS, and toluene obtained using the fabricated portable system with 10 mW laser power and 5 s integration time. All the spectra are normalized along the y axis. The vertical dotted lines represent the lower cutoff region (700 cm^{-1}) for the fabricated system imposed by the 550 nm long-pass filter.

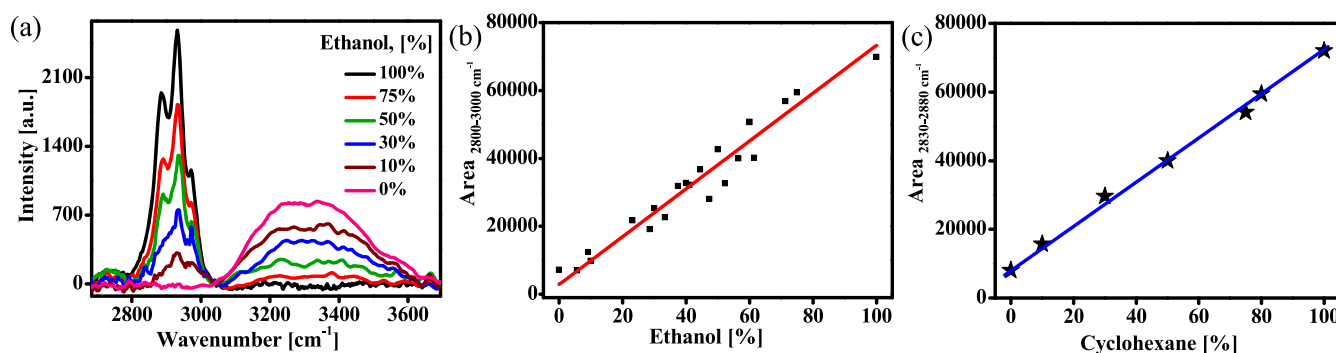


Figure 4. (a) Raman spectra in the range 2700–3700 cm^{-1} of ethanol–water mixtures of varying compositions collected using the device with 10 mW laser power and 5 s integration time. The spectra were averaged over three accumulations and baseline corrected using a moving point average method.⁴⁰ (b) Variation in integrated peak intensity in the range 2800–3000 cm^{-1} vs ethanol concentration and (c) variation in integrated peak intensity in the range 2830–2880 cm^{-1} vs cyclohexane concentration for cyclohexane–toluene mixtures.

tabulated in the [Supporting Information](#) and were assigned to specific bond vibrations from literature references.^{43–48}

In general, for all the compounds investigated, we found good agreements between data obtained from the fabricated device and commercial system in terms of spectral band position and relative intensities. For example, the dominant peaks observed with the fabricated spectrometer system for benzonitrile were 1014 cm^{-1} , 1612 cm^{-1} , 2243 cm^{-1} , and 3075 cm^{-1} arising from the C–C stretch/ring breath, C=C stretch, C–N stretch, and C–H stretch vibrations, respectively. Our spectrometer's lower spectral acquisition limit is $\sim 700 \text{ cm}^{-1}$ because we have employed a 550 nm long-pass filter. The other apparent difference was with the spectral resolution. Very close peaks (751.3 cm^{-1} and 767.1 cm^{-1} , 1007 cm^{-1} and 1026.6 cm^{-1} , and 1177.7 cm^{-1} and 1192.6 cm^{-1}) whose separation was less than 30 cm^{-1} appeared as single peaks in the Raman spectrum acquired with the currently fabricated system. This is mainly limited by the FWHM of the laser and the resolution of the spectrometer, which resulted in minor variation in the spectral band position with respect to the reported values, see [Supporting Information](#). The other factors contributing to this could be inaccuracies in determining the exact wavelength of the excitation source.

Chemical Mixture Analysis

As the obtained Raman spectral intensities are functions of excitation power, scattering cross-section of the sample, and the material's concentration in the sample, the technique can be used for quantitative analysis. In effect, the observed Raman spectrum will be the algebraic sum of the individual components' contributions. To illustrate the current system's potential for mixture analysis, we studied two model systems: (i) ethanol blended with water and (ii) a cyclohexane–toluene mixture. For the ethanol–water combination, 16 mixtures were created in the concentration range 0–100 volume percentage, and the acquired spectra after baseline correction are presented in [Figure 4a](#). The characteristic Raman peaks for water due to OH stretching appeared in the range 3100–3600 cm^{-1} , while CH₃–CH₂ stretching of ethanol peaked in the range ~ 2800 –3000 cm^{-1} .⁴⁷ The analysis of the data revealed a linear variation in the integrated peak intensities against ethanol concentration. [Figure 4b](#) shows the plot of integrated peak intensity (area under the peak) in the range 2800–3000 cm^{-1} against the ethanol volume percentage. The linear fit ($y = mx + c$) of this graph yielded a correlation coefficient R^2 value of 0.97. Instead of peak area, one could also employ the peak

intensity for generating a calibration graph; however, there will be a diminished correlation with concentration, as shown in the [Supporting Information](#). In 2001, Sanford et al. attempted to quantify ethanol from alcoholic beverages using a modular Raman system composed of an argon ion laser as the excitation source and Ocean Optics S-2000 CCD detector.¹⁷ Their design also involves using two additional parabolic mirrors, the first one to reflect the transmitted laser light to the sample, thereby increasing the Raman scattering efficiency, and the second to reflect any backscattered signal to the collection optics. As a result, they have obtained a very good R^2 value of 0.9978 for the calibration graph, and the estimated detection limit was 1%.

Similar results obtained for cyclohexane–toluene mixtures are shown in the [Supporting Information](#). The integrated peak intensity in the range 2830–2880 cm^{-1} (CH₂ stretching of cyclohexane) varied linearly with changes in the composition of mixtures. The R^2 value of the linear fit was estimated to be 0.99.

Effect of Laser Power

We studied the effect of excitation power to identify the minimum required laser intensity for producing a detectable signal with the current Raman spectrometer. Raman spectra of benzonitrile recorded by varying laser power from 5 mW to 55 mW are presented in the [Supporting Information](#). It could be noticed that with the present configuration, the Raman signals were clear and distinguishable at excitation powers as small as 5 mW. Thus, these results indicate adaptability of the current design with lower power laser pointers (<10 mW), as illustrated in some of the prior arts (see [Table 1](#) and refs 31, 33, and 34), which help to improve the safety substantially for classroom demonstration.

Student Learning Outcome

The student learning outcome was assessed on undergraduate and graduate students who visited our laboratory as part of summer programs and those at the early stages of their research program. The students were first introduced to the basic concepts of light-matter interaction, RS, and the spectrometer's operating principles by familiarizing components and their functions. Students were given different sets of samples such as benzonitrile, ethanol, cyclohexane, jewelry containing diamonds, and medicinal paracetamol tablets (contains acetaminophen as the single API) along with a library of reference spectra ([Supporting Information](#)). More than 98% of the students could accurately establish the

unknown samples' identity, and 70% could successfully assign the observed peaks to specific bond vibrations. Research students were provided with the task of configuring the device with collection optics of different numerical apertures (NA) and identifying the effect of NA on the observed Raman spectrum. The students reported almost 4 times higher signal intensity while using an objective lens (Holmarc HO-PA-MO20X) with an NA of 0.4 than with a standard convex lens of focal length 30 mm and aperture 25 mm (see Supporting Information).

Additionally, we conducted a live demonstration of the spectrometer and lectures of 1 h duration in a few selected colleges. Each of these sessions was attended by more than 40 students.

SUMMARY AND FURTHER WORK

In summary, the design and fabrication of a cost-effective portable Raman spectrometer are presented here. The simplicity of the fabrication procedures detailed herein and the nominal cost of materials make it easily achievable at any educational institution. The design strategy provided in the manuscript offers the flexibility of configuring Raman systems with a different excitation wavelength, and the only modification to be implemented will be the choice of the long-pass filter with the right cutoff wavelength. This helps to explore other capabilities of RS. For example, configuring the system with 405 nm allows study of the well-known resonance Raman effect, which provides a 10^6 signal enhancement with biologically important molecules such as heme and chlorophyll. On the other hand, configuring it with a longer wavelength laser diode (e.g., 650 nm) will help record the Raman spectrum with reduced fluorescence. Yet, another possibility is to explore the demonstration of the concept of SERS with easily preparable metal nanoparticle solutions,^{48–50} which yield enhancement factors as high as 10^{10} .

ASSOCIATED CONTENT

Supporting Information

The Supporting Information is available at <https://pubs.acs.org/doi/10.1021/acs.jchemed.0c01028>.

Details of the optical components; photographs of the stage-wise fabrication procedures; specifications of the confocal Raman microscope; comparison of spectra from confocal Raman microscope and fabricated system; fabrication steps of the home-built Czerny turner spectrometer and its calibration procedure; data of influence of laser power; data of mixture analysis; and student learning outcomes (PDF)

AUTHOR INFORMATION

Corresponding Author

Karuvath Yoosaf – Photosciences and Photonics Section, Chemical Sciences and Technology Division, CSIR-National Institute for Interdisciplinary Science and Technology, Thiruvananthapuram 695019, Kerala, India; Academy of Scientific and Innovative Research (AcSIR), Ghaziabad 201002, India; orcid.org/0000-0002-8837-4490; Email: yoosafk@niist.res.in

Authors

Neethu Emmanuel – Photosciences and Photonics Section, Chemical Sciences and Technology Division, CSIR-National Institute for Interdisciplinary Science and Technology, Thiruvananthapuram 695019, Kerala, India; Academy of Scientific and Innovative Research (AcSIR), Ghaziabad 201002, India; orcid.org/0000-0002-2463-0467

Raji B Nair – Photosciences and Photonics Section, Chemical Sciences and Technology Division, CSIR-National Institute for Interdisciplinary Science and Technology, Thiruvananthapuram 695019, Kerala, India; orcid.org/0000-0003-1257-4987

Bini Abraham – Photosciences and Photonics Section, Chemical Sciences and Technology Division, CSIR-National Institute for Interdisciplinary Science and Technology, Thiruvananthapuram 695019, Kerala, India; orcid.org/0000-0002-1694-4204

Complete contact information is available at: <https://pubs.acs.org/10.1021/acs.jchemed.0c01028>

Notes

The authors declare no competing financial interest.

ACKNOWLEDGMENTS

The authors wish to acknowledge Ms/Vinivish Technologies Pvt. Ltd., Thiruvananthapuram, and KSCSTE for partial funding through the KSCSTE-VINVISH-NIIST PAIR program for this project. Funding was also provided by CSIR-Mission mode (HCP 0012), CSIR-Fast Track Translation (MLP 0039), and DBT (BT/PR22475/NNT/28/1193/2016) projects. This is contribution No. NIIST/2019/Nov/61 from CSIR-National Institute for Interdisciplinary Science and Technology, Thiruvananthapuram.

REFERENCES

- (1) Raman, C. V.; Krishnan, K. S. A new class of spectra due to secondary radiation. *Indian J. Phys.* **1928**, *2*, 379–396.
- (2) Kong, K.; Kendall, C.; Stone, N.; Notingher, I. Raman spectroscopy for medical diagnostics From in-vitro biofluid assays to in-vivo cancer detection. *Adv. Drug Delivery Rev.* **2015**, *89*, 121–134.
- (3) Synytsya, A.; Judexova, M.; Hoskovec, D.; Miskovicova, M.; Petruzalka, L. Raman spectroscopy at different excitation wavelengths (1064, 785 and 532 nm) as a tool for diagnosis of colon cancer. *J. Raman Spectrosc.* **2014**, *45* (10), 903–911.
- (4) Li, Y.; Igne, B.; Drennen, J. K.; Anderson, C. A. Method development and validation for pharmaceutical tablets analysis using transmission Raman spectroscopy. *Int. J. Pharm.* **2016**, *498* (1–2), 318–325.
- (5) Herrero, A. M. Raman spectroscopy a promising technique for quality assessment of meat and fish: A review. *Food Chem.* **2008**, *107* (4), 1642–1651.
- (6) Ong, T. T. X.; Blanch, E. W.; Jones, O. A. H. Surface Enhanced Raman Spectroscopy in environmental analysis, monitoring and assessment. *Sci. Total Environ.* **2020**, *720*, 137601.
- (7) Izake, E. L.; Cletus, B.; Olds, W.; Sundarajoo, S.; Fredericks, P. M.; Jaatinen, E. Deep Raman spectroscopy for the non-invasive standoff detection of concealed chemical threat agents. *Talanta* **2012**, *94*, 342–349.
- (8) Izake, E. L. Forensic and homeland security applications of modern portable Raman spectroscopy. *Forensic Sci. Int.* **2010**, *202* (1–3), 1–8.
- (9) Cui, Y.; Phang, I. Y.; Lee, Y. H.; Lee, M. R.; Zhang, Q.; Ling, X. Y. Multiplex plasmonic anti-counterfeiting security labels based on

surface-enhanced Raman scattering. *Chem. Commun.* **2015**, *51* (25), 5363–5366.

(10) Edwards, H. G. M. Chapter 5 - Raman Spectroscopy in Art and Archaeology: A New Light on Historical Mysteries. In *Frontiers of Molecular Spectroscopy*; Laane, J., Ed.; Elsevier: Amsterdam, 2009; pp 133–173.

(11) Xi, S.; Zhang, X.; Du, Z.; Li, L.; Wang, B. Z.; Luan, Z.; Lian, C.; Yan, J. Y. Laser Raman detection of authigenic carbonates from cold seeps at the Formosa Ridge and east of the Pear River Mouth Basin in the South China Sea. *J. Asian Earth. Sci.* **2018**, *168*, 207–224.

(12) O'Brien, L. C.; Kubicek, R. L.; O'Brien, J. J. Laser Raman Spectroscopy of Diamond. *J. Chem. Educ.* **1994**, *71* (9), 759–760.

(13) Aponick, A.; Marchozzi, E.; Johnston, C. R.; Wigal, C. T. Determining the Authenticity of Gemstones Using Raman Spectroscopy. *J. Chem. Educ.* **1998**, *75* (4), 465–466.

(14) Frey, E. R.; Sygula, A.; Hammer, N. I. Particle in a Disk: A Spectroscopic and Computational Laboratory Exercise Studying the Polycyclic Aromatic Hydrocarbon Corannulene. *J. Chem. Educ.* **2014**, *91* (12), 2186–2190.

(15) Adams, W.; Sonntag, M. D. Vibrational Spectroscopy of Hexynes: A Combined Experimental and Computational Laboratory Experiment. *J. Chem. Educ.* **2018**, *95* (7), 1205–1210.

(16) Nielsen, S. E.; Scaffidi, J. P.; Yezierski, E. J. Detecting Art Forgeries: A Problem-Based Raman Spectroscopy Lab. *J. Chem. Educ.* **2014**, *91* (3), 446–450.

(17) Sanford, C. L.; Mantooh, B. A.; Jones, B. T. Determination of Ethanol in Alcohol Samples Using a Modular Raman Spectrometer. *J. Chem. Educ.* **2001**, *78* (9), 1221–1225.

(18) Craig, N. C.; Fuchsman, W. H.; Lacuesta, N. N. Investigation of Model Cell Membranes with Raman Spectroscopy: A Biochemistry Laboratory Experiment. *J. Chem. Educ.* **2003**, *80* (11), 1282–1288.

(19) Wang, L.; Mizaikoff, B.; Kranz, C. Quantification of Sugar Mixtures with Near-Infrared Raman Spectroscopy and Multivariate Data Analysis. A Quantitative Analysis Laboratory Experiment. *J. Chem. Educ.* **2009**, *86* (11), 1322–1325.

(20) Pavel, I. E.; Alnajjar, K. S.; Monahan, J. L.; Stahler, A.; Hunter, N. E.; Weaver, K. M.; Baker, J. D.; Meyerhoefer, A. J.; Dolson, D. A. Estimating the Analytical and Surface Enhancement Factors in Surface-Enhanced Raman Scattering (SERS): A Novel Physical Chemistry and Nanotechnology Laboratory Experiment. *J. Chem. Educ.* **2012**, *89* (2), 286–290.

(21) Basu-Dutt, S.; Minus, M. L.; Jain, R.; Nepal, D.; Kumar, S. Chemistry of Carbon Nanotubes for Everyone. *J. Chem. Educ.* **2012**, *89* (2), 221–229.

(22) Parobek, D.; Shenoy, G.; Zhou, F.; Peng, Z.; Ward, M.; Liu, H. Synthesizing and Characterizing Graphene via Raman Spectroscopy: An Upper-Level Undergraduate Experiment That Exposes Students to Raman Spectroscopy and a 2D Nanomaterial. *J. Chem. Educ.* **2016**, *93* (10), 1798–1803.

(23) Masson, J.-F.; Yockell-Lelièvre, H. Spectroscopic and Physical Characterization of Functionalized Au Nanoparticles: A Multiweek Experimental Project. *J. Chem. Educ.* **2014**, *91* (10), 1557–1562.

(24) McMillan, B. G. Achieving Very Low Levels of Detection: An Improved Surface-Enhanced Raman Scattering Experiment for the Physical Chemistry Teaching Laboratory. *J. Chem. Educ.* **2016**, *93* (10), 1804–1808.

(25) Mayhew, H. E.; Frano, K. A.; Svoboda, S. A.; Wustholz, K. L. Using Raman Spectroscopy and Surface-Enhanced Raman Scattering To Identify Colorants in Art: An Experiment for an Upper-Division Chemistry Laboratory. *J. Chem. Educ.* **2015**, *92* (1), 148–152.

(26) Galloway, D. B.; Ciolkowski, E. L.; Dallinger, R. F. Raman spectroscopy for the undergraduate physical and analytical laboratories. *J. Chem. Educ.* **1992**, *69* (1), 79.

(27) Sutherland, W. S.; Alarie, J. P.; Stokes, D. L.; Vo-Dinh, T. A Portable Surface-Enhanced Raman Spectrometer. *Instrum. Sci. Technol.* **1994**, *22* (3), 231–239.

(28) Fitzwater, D. A.; Thomasson, K. A.; Glinski, R. J. A Modular Raman Spectroscopy System Using a Helium-Neon Laser That Is

Also Suited for Emission Spectrophotometry Experiments. *J. Chem. Educ.* **1995**, *72* (2), 187.

(29) Bandyopadhyay, A. K.; Dilawar, N.; Vijayakumar, A.; Varandani, D.; Singh, D. A low cost laser-Raman spectrometer. *Bull. Mater. Sci.* **1998**, *21* (5), 433–438.

(30) DeGraff, B. A.; Hennip, M.; Jones, J. M.; Salter, C.; Schaertel, S. A. An Inexpensive Laser Raman Spectrometer Based on CCD Detection. *Chem. Educ.* **2002**, *7* (1), 15–18.

(31) Young, M. A.; Stuart, D. A.; Lyandres, O.; Glucksberg, M. R.; Van Duyne, R. P. Surface-enhanced Raman spectroscopy with a laser pointer light source and miniature spectrometer. *Can. J. Chem.* **2004**, *82* (10), 1435–1441.

(32) Johnson, D.; Larsen, P.; Fluellen, J.; Furton, D.; Schaertel, S. A. A Modular Raman Spectrometer for Solids. *Chem. Educ.* **2008**, *13* (2), 82–86.

(33) Mohr, C.; Spencer, C. L.; Hippler, M. Inexpensive Raman Spectrometer for Undergraduate and Graduate Experiments and Research. *J. Chem. Educ.* **2010**, *87* (3), 326–330.

(34) Somerville, W. R. C.; Le Ru, E. C.; Northcote, P. T.; Etchegoin, P. G. High performance Raman spectroscopy with simple optical components. *Am. J. Phys.* **2010**, *78* (7), 671–677.

(35) Montoya, E. H.; Arbildo, A.; Baltuano, O. R. A Homemade Cost Effective Raman Spectrometer with High Performance. *J. Lab. Chem. Educ.* **2015**, *3* (4), 67–75.

(36) Griffiths, P. R. Introduction to the Theory and Instrumentation for Vibrational Spectroscopy. In *Handbook of Vibrational Spectroscopy*; John Wiley & Sons, Ltd.; 2010.

(37) Spieler, H. Silicon Detectors Many Different Applications, but Built on the Same Basic Physics. IEEE 2012 Nuclear Science Symposium, Medical Imaging Conference, Anaheim, California, 2012.

(38) Kovarik, M. L.; Clapis, J. R.; Romano-Pringle, K. A. Review of Student-Built Spectroscopy Instrumentation Projects. *J. Chem. Educ.* **2020**, *97* (8), 2185–2195.

(39) Rossel, E. TCD1304 PCB. <https://tcd1304.wordpress.com/tcd1304-pcb/> (accessed 3/28/2021).

(40) Krishna, H.; Majumder, S. K.; Gupta, P. K. Range-independent background subtraction algorithm for recovery of Raman spectra of biological tissue. *J. Raman Spectrosc.* **2012**, *43* (12), 1884–1894.

(41) University of Georgia Office of Research. Research Safety: Laser Safety Guidelines. <https://research.uga.edu/safety/laser/safety/> (accessed 3/28/2021).

(42) Laser Institute of America. American National Standards Institute—Z136.5: Safe Use of Lasers in Educational Institutions. <https://www.lia.org/resources/laser-safety-information/laser-safety-standards/ansi-z136-standards/z136-5> (accessed 3/28/2021).

(43) McCreery, R. L. *Raman Spectroscopy for Chemical Analysis*; John Wiley & sons: Canada, 2000.

(44) Cai, D.; Neyer, A.; Kuckuk, R.; Heise, H. M. Raman, mid-infrared, near-infrared and ultraviolet–visible spectroscopy of PDMS silicone rubber for characterization of polymer optical waveguide materials. *J. Mol. Struct.* **2010**, *976* (1), 274–281.

(45) Yadav, R. A.; Singh, I. S. Vibrational spectra and normal coordinate analysis for substituted trifluoromethyl benzenes. *J. Chem. Sci.* **1985**, *95* (5), 471–487.

(46) Borjanovic, V.; Bistričić, L.; Vlasov, I.; Furić, K.; Zamboni, I.; Jaksic, M.; Shenderova, O. Influence of proton irradiation on the structure and stability of poly(dimethylsiloxane) and poly-(dimethylsiloxane)-nanodiamond composite. *J. Vac. Sci. Technol.* **2009**, *27* (6), 2396–2403.

(47) Numata, Y.; Iida, Y.; Tanaka, H. Quantitative analysis of alcohol-water binary solutions using Raman spectroscopy. *J. Quant. Spectrosc. Radiat. Transfer* **2011**, *112* (6), 1043–1049.

(48) Emmanuel, N.; Haridas, R.; Chelakkar, S.; Nair, R. B.; Gopi, A.; Sajitha, M.; Yoosaf, K. Smartphone Assisted Colourimetric Detection and Quantification of Pb²⁺ and Hg²⁺ Ions Using Ag Nanoparticles from Aqueous Medium. *IEEE Sens. J.* **2020**, *20* (15), 8512–8519.

(49) Yoosaf, K.; Ipe, B. I.; Suresh, C. H.; Thomas, K. G. In Situ Synthesis of Metal Nanoparticles and Selective Naked-Eye Detection

of Lead Ions from Aqueous Media. *J. Phys. Chem. C* **2007**, *111* (34), 12839–12847.

(50) Sajitha, M.; Vindhyasarumi, A.; Gopi, A.; Yoosaf, K. Shape controlled synthesis of multi-branched gold nanocrystals through a facile one-pot bifunctional biomolecular approach. *RSC Adv.* **2015**, *5* (119), 98318–98324.